Title: Simultaneous fat-free isotropic 3D anatomical imaging and Tlt;subgt;2lt;/subgt; mapping of knee cartilage with lipid-insensitive binomial off-resonant RF excitation (LIBRE) pulses.

Authors: Colotti R, Omoumi P, van Heeswijk RB, Bastiaansen JAM

Journal: Journal of magnetic resonance imaging : JMRI

Year: 2019 May

Issue: 49

Volume: 5

Pages: 1275-1284

DOI: 10.1002/jmri.26322

Simultaneous Fat-Free Isotropic 3D Anatomical Imaging and T_2 Mapping of Knee Cartilage with Lipid Insensitive Binomial Off-Resonant RF Excitation (LIBRE) Pulses

Roberto Colotti[1], Patrick Omoumi[1], Ruud B. van Heeswijk[1,2*], and Jessica A.M. Bastiaansen[1*]

*** These authors contributed equally**

[1]Department of Radiology, University Hospital (CHUV) and University of Lausanne (UNIL), Lausanne, Switzerland

[2]Centre for Biomedical Imaging (CIBM), Lausanne, Switzerland

ABSTRACT

Background: Improved knee cartilage morphological delineation and T_2 mapping precision necessitates isotropic 3D high-resolution and efficient fat suppression.

Purpose: To develop and assess an isotropic 3D lipid-insensitive T_2 mapping technique of the knee for improved cartilage delineation and precise measurement of T_2 relaxation times.

Study Type: Prospective.

Phantom/Subjects: Phantoms (n=6) used in this study were designed to mimic the T_1 and T_2 relaxation times of cartilage and fat. The study cohort comprised healthy volunteers (n=7) for morphometry and T_2 relaxation time measurements.

Field Strength/Sequence: High resolution isotropic 3D T_2 mapping technique that uses sequential T_2-prepared segmented gradient-recalled echo (Iso3DGRE) images and lipid-insensitive binomial off-resonant RF excitation (LIBRE) at 3T.

Assessment: Numerical simulations and phantom experiments were performed to optimize the LIBRE pulse. Phantom studies were carried out to test the accuracy of the technique against reference standard spin-echo (SE) T_2 mapping. Subsequently, T_2 maps with and without LIBRE pulses were acquired in knees of healthy volunteers and the T_2 relaxation time values in different cartilage compartments were compared.

Statistical Tests: A two-tailed paired Student's t-test was used to compare the average T_2 values and the relative standard deviations (inverse measurement of the precision) obtained with and without LIBRE pulses.

Results: A LIBRE pulse of 1ms suppressed fat with a radiofrequency (RF) excitation frequency offset of 1560Hz and optimal RF excitation angle of 35°. These results were

corroborated by phantom and knee experiments. Robust and homogeneous fat suppression was obtained (a fat SNR decrease of 86.4±2.4%). In phantoms, T_2-values were found in good agreement when comparing LIBRE-Iso3DGRE with SE (slope 0.93±0.04, intercept 0.11±1.6ms, R^2>0.99). In vivo, LIBRE excitation resulted in more precise T_2 estimation (23.7±7.4%) than normal excitation (30.5±9.9%, P<0.0001).

Data Conclusion: Homogeneous LIBRE fat signal suppression was achieved with a total RF pulse duration of 1ms, allowing for the removal of chemical shift artifacts and resulting in improved cartilage delineation and precise T_2 values.

Key words: Knee cartilage; T_2 mapping; Water excitation; Fat suppression

INTRODUCTION

Progressive cartilage degeneration is considered one of the hallmarks of osteoarthritis (OA), a common condition that affects the joints and for which, so far, no effective cure has been found (1). Rising obesity and the aging trend of the world population will likely worsen the future prevalence of the disease, which in 2010 was already estimated to affect 3.8% of the global population(2) .

Cartilage has a limited capacity to regenerate, which makes it crucial to detect OA at an early stage, before any permanent cartilage tissue loss. Several compositional magnetic resonance imaging (MRI) techniques have been proven effective in quantifying and characterizing cartilage composition at both the biochemical (3) and ultrastructural level (4). Given the correlation between the T_2 relaxation time and the increase in free water mobility that occurs in cartilage during the early stages of the disease, T_2 mapping is considered as a sensitive quantitative technique for the detection of early OA changes (5). T_2 mapping has therefore gained increasing interest as an outcome measure in research (6,7) and is also used in clinical routine (8).

T_2 mapping techniques can be based on both two-dimensional (2D) or on three-dimensional (3D) pulse sequences, such as dual-echo spin echo (SE) (9), multi-slice multi-echo spin echo (MSME) (10), double-echo steady state (DESS) (11), triple-echo steady state (TESS) (12) and spoiled gradient echo (13). Two-dimensional techniques have limited spatial coverage and often have poor through-slice resolution, which may cause partial-volume effects that do not allow the evaluation of specific regions affected by the disease. In order to overcome these limitations, 3D techniques have been developed to attain 1) higher signal-to-noise ratio (SNR) efficiency that results in improved

precision in T_2 estimation, 2) wider coverage of the joint under examination, and 3) a higher spatial resolution in the third dimension. However, such 3D techniques usually come at the cost of a significant increase in scan time.

Recently, a submillimetric isotropic 3D T_2 mapping technique of knee cartilage (Iso3DGRE) (14) with a clinically feasible acquisition time (usually up to a dozen of minutes for the knee)(15,16) has been developed and validated. Its isotropic nature allows for reformats in any plane and minimization of partial volume effects, which results in a more accurate T_2 relaxation time quantification.

In addition to partial volume effects, the accuracy of knee cartilage T_2 mapping is also often affected by fat signal from the subchondral bone that is shifted onto the cartilage due to their chemical shift (CS) differences, and this may especially be pronounced when acquisitions are performed at low receiver bandwidth to increase SNR. Therefore, a robust and time-efficient fat suppression would greatly enhance the delineation and accuracy of cartilage T_2 mapping.

Commonly used fat suppression techniques (17) typically exploit the differences in the fat and water T_1 relaxation times (18), Larmor frequencies (19), or both (20). Using inversion recovery pulses that exploit the T_1 differences to achieve fat saturation directly results in prolonged scan durations (18). Similarly, the performance of conventional binomial water excitation (WE) pulses increases with the number of sub-pulses, at the expense of RF pulse duration. In general, all WE methods are characterized by a compromise between RF pulse durations and thus scan time, specific absorption rate (SAR), and the sensitivity to magnetic field (B_0) inhomogeneities and radiofrequency (RF) pulse (B_1) imperfections. Recently, a novel WE RF pulse that is robust to both B_0 and B_1 inhomogeneities and that allows for a homogeneous fat suppression with a large bandwidth has been developed

and validated at 3T. This lipid-insensitive binomial off-resonant RF excitation (LIBRE) pulse (21) was demonstrated for a range of pulse durations from 1.4 to 2.6ms and was shown to enable superior fat suppression compared to conventional WE and fat saturation techniques, both in terms of SNR and insensitivity to magnetic field inhomogeneities. However, the utilization of the LIBRE pulse in knee musculoskeletal applications has not been explored yet.

The aim of the current study was first to develop and characterize a shortened version of the LIBRE pulse with a duration of 1ms, and then to combine it with the recently proposed Iso3DGRE T_2 mapping technique, in order to create an isotropic 3D lipid-insensitive T_2 mapping technique of knee cartilage (LIBRE-Iso3DGRE). The technique was then validated in phantoms and in healthy volunteers at 3T.

MATERIAL AND METHODS

LIBRE pulse optimization

The LIBRE pulse is composed of two rectangular sub-pulses that have an RF frequency offset (f_{RF}), sub-pulse duration (τ) and a specific phase offset ($\varphi=2\pi f\tau$) between the first and the second sub-pulse. This variable parameter space was exploited to achieve robust fat suppression with total pulse duration of 1ms (i.e. 2τ). When a single rectangular sub-pulse produces a 2π rotation of the fat magnetization vector (and thus allowing for fat signal suppression), the relation between f_{RF}, the resonance frequency of fat (f_{fat}), the RF excitation angle (α) and τ can be described by (21):

$$\tau = \frac{\sqrt{1-(\alpha/2\pi)^2}}{\Delta f + \gamma \Delta B_0} \quad (\mathrm{Eq.}\,1),$$

where Δf is the difference between f_{RF} and f_{fat} at 3T, ΔB_0 represents the local magnetic field inhomogeneity and α is in radians. In the absence of field inhomogeneities ($\Delta B_0=0$) and assuming small RF excitation angles, the optimal f_{RF} (f_{RFopt}) can be straightforwardly calculated.

Bloch equation simulations (22) were performed in Matlab (The MathWorks, Natick, Massachusetts, USA) to determine the optimal α (α_{opt}) that resulted in simultaneous fat suppression and water excitation. The T_1 and T_2 relaxation times were assumed to be 1320ms and 38ms respectively (similar to those of healthy cartilage (23)). Additional parameters included a segmented k-space gradient-echo (GRE) acquisition with 100 excitations per segment, a T_2 preparation module (T_2prep) (24) with a duration (TE_{T2prep}) of 53ms, a repetition time (TR) of 7.1ms and an echo time (TE) of 3.2ms. Total LIBRE pulse duration was set to 1ms, and the transverse magnetization (M_{xy}) was characterized as a function of α and tissue frequency, with water resonating at 0Hz and fat at -440Hz when using a magnetic field strength of 3T.

Given the off-resonance excitation with LIBRE, the RF excitation angle α at the offset f_{RF} allows for the optimal excitation of water protons: the actual rotation angle of water equals the Ernst angle, and was the same for both pulse sequences used in this study. This parameter, therefore, is not dependent on TE_{T2prep}, TR, T_1, or T_2, but it mostly depends on f_{RF}, which defines the extent of the off-resonance excitation.

MR protocols and T_2 fitting model

All experiments were performed on a 3T clinical system (Magnetom Prisma, Siemens Healthcare, Erlangen, Germany) with a 15-channel Tx/Rx knee coil (Quality Electrodynamics, Mayfield, Ohio, USA). Iso3DGRE pulse sequence parameters with and

without LIBRE excitation pulse (and thus with and without fat suppression capability) are reported in Table 1. The pulse sequence diagram, together with the RF pulse design are depicted in the Supplementary Material (Supporting Figure S1). A least-square method was used in Matlab to perform pixel-wise T_2 mapping. As previously established (25-27), an empirical offset was added to the T_2-fitting equation in order to compensate for T_1 recovery during the relatively long segmental acquisition time and was set to enhance sensitivity to T_2 relaxation time in order to increase the accuracy of the fit (14) as follows:

$$S\left(TE_{T2prep}\right) = S_0 \cdot \left[e^{\frac{-TE_{T2prep}}{T_2}} + \frac{\delta}{T_2}\right] \quad (Eq.\,2),$$

where S_0 is defined as the signal when TE_{T2prep} is zero and δ represents the empirical offset. The T_2-fitting offset δ was empirically chosen such that the intercept value in the linear regression between the gold standard spin echo (SE) (28) and the LIBRE-Iso3DGRE phantom T_2 values was minimized and the linear regression slope was closest to 1.

In vitro characterization

Phantom studies were performed in order to verify the optimized LIBRE parameters f_{RFopt} and α_{opt}, to determine the empirical fit offset, to characterize the accuracy of the technique against the gold standard SE and finally to compare the T_2 relaxation time estimation obtained with normal excitation and with the LIBRE pulse (Iso3DGRE vs. LIBRE-Iso3DGRE).

The phantoms used in this study were designed to mimic the T_1 and T_2 relaxation times of cartilage and fat. To this end, five tubes with mixed solutions of agar (3-5% w/v) and 0.73μM $NiCl_2$ and a tube of baby oil (Johnson and Johnson, New Brunswick, New Jersey,

USA) were built. Given the use of GeneRalized Autocalibrating Partially Parallel Acquisitions (GRAPPA) (29), the signal-to-noise ratio (SNR) was approximated as the ratio between the signal in a region of interest (ROI) drawn within the phantoms and the standard deviation of the noise in an ROI of at least 20×20 pixels well outside the object of interest (30).

A series of low-resolution LIBRE-Iso3DGRE scans with varying f_{RF} (from 1500 to 1700Hz) were performed to confirm f_{RFopt}. Additional sequence parameters are reported in Table 1. To verify α_{opt}, the above-mentioned phantoms were scanned with LIBRE-Iso3DGRE and with α varying from 5° to 40°. The 4% agar phantom, which has T_1 and T_2 relaxation times similar to those of healthy cartilage, was used for data analysis.

The optimized LIBRE-Iso3DGRE protocol was then used to acquire the four input images (TE_{T2prep}=0-23-38-53ms) that are needed in order to calculate a T_2 map. TE_{T2prep}=23ms was the minimum possible duration of the T_2 preparation module, which was incremented in steps of 15ms to cover the physiological range of cartilage T_2 values and to maximize T_2 fitting precision (27). The empirical fit offset was chosen to minimize the intercept value in the linear regression between the SE and the LIBRE-Iso3DGRE T_2 values. The SE sequence was performed with the following parameters TR=7000ms, TE=6.8-15-30-60-120-250-400ms, field of view (FOV)=250×132mm^2, matrix size=192×92, one slice with slice thickness (ST)=6mm.

The T_2 map of the phantoms was then used to compare the accuracy of the LIBRE-Iso3DGRE technique against SE and to evaluate the difference in T_2 estimation obtained with Iso3DGRE and LIBRE-Iso3DGRE.

The approximate SNR in the 4% agar phantom and in the fat compartment was measured and compared between LIBRE water excitation and conventional WE (1-180°-1) pulse (31) and spectral fat saturation (19).

Healthy volunteer studies

In vivo studies were approved by the Institutional Review Board (IRB) and written informed consent was obtained from all volunteers before each scan. The knees of seven healthy volunteers (five men and two women; average age 26.7±3.5years; age range 22–33years; body mass index (BMI) 22.5±4.0kg/m^2) were scanned with LIBRE-Iso3DGRE and Iso3DGRE pulse sequences and T_2 maps were generated. None of the volunteers had a history of knee trauma or surgery, pain or swelling.

Six continuous slices that covered the central region of the lateral and medial condyles were chosen for analysis. Eight cartilage sub-compartments were defined on the sagittal plane (femoral lateral anterior, femoral lateral central, femoral lateral posterior, lateral tibial, femoral medial anterior, femoral medial central, femoral medial posterior, medial tibial). The anterior and posterior margins of, respectively, the anterior and posterior menisci were used as hallmarks to differentiate between the central and the anterior/posterior femoral compartment. For each subject, the images acquired with the LIBRE-Iso3DGRE pulse sequence and TE_{T2prep}=23ms were used for segmentation. The same ROIs were then used for the Iso3DGRE T_2 maps. ROIs were manually drawn in Matlab by a research assistant (--, with 4 years of experience) under the supervision of a musculoskeletal radiologist (--, with 9 years of experience). Positioning cushions, whose

air volume was inflated with a hand pump, were used to avoid knee movement and to minimize misregistration errors.

Both LIBRE-Iso3DGRE and Iso3DGRE T_2 maps were visually inspected for apparent differences in anatomical patterns. The presence of CS artifacts was visually assessed and was classified according to the following scale: completely absent - reduced - unchanged.

For each subject, the approximate SNR was measured in the femoral bone marrow and in the infrapatellar fat pad fat compartments. For both T_2 mapping techniques, the images acquired with TE_{T2prep}=0ms were used for SNR analysis.

SAR values were recorded during both LIBRE-Iso3DGRE and Iso3DGRE acquisitions for all volunteers.

Statistical analysis

Statistical analysis was performed with GraphPad Prism 6.0 (GraphPad Software, La Jolla, California, USA).

For both in vitro and in vivo studies, the mean T_2 value was calculated with its standard deviation in each ROI.

For in vitro studies, the accuracy of the LIBRE-Iso3DGRE technique was evaluated against the gold standard SE using a linear regression and Bland-Altman analysis (32). The difference in phantom T_2 values obtained with LIBRE-Iso3DGRE and Iso3DGRE was ascertained by performing a Bland-Altman analysis.

For healthy volunteer studies, T_2 values above 100ms (i.e. synovial fluid pixels) and below 0ms (i.e. poor fit pixels) were excluded from the analysis. Extreme outliers were also excluded, as previously reported (14). A two-tailed paired Student’s t-test was used to

evaluate the difference in compartmental T_2 values between the LIBRE-Iso3DGRE and Iso3DGRE T_2 mapping techniques. The precision was defined as the inverse of the relative standard deviation (the ratio of the standard deviation and the average T_2 value within the ROIs) and was compared between the two techniques using a paired two-tailed Student's t-test. Statistical significance was set as $P<0.05$.

RESULTS

LIBRE pulse characterization

In the absence of B_0 inhomogeneities and small RF excitation angles, a LIBRE pulse of 1ms suppressed fat with a f_{RFopt} of 1560Hz (Eq. 1). The M_{xy} simulations following a T_2 preparation module of 53ms and a LIBRE excitation pulse (RF frequency offset of 1560Hz, sub-pulse duration of 0.5ms) showed maximized water excitation and a fat suppression bandwidth of ~100 Hz at α=35° (i.e. α_{opt}, Figure 1a).

Phantom studies

The numerically obtained α_{opt} of 35° also resulted in the maximum obtained water SNR in the agar phantom (Figure 1b). The images furthermore demonstrated a complete signal suppression of the fat phantom (SNR=28.6) when using a numerically optimized LIBRE pulse of 1ms and f_{RFopt} of 1560 Hz (Figure 1c). The numerical simulations (Fig. 1a) were thus confirmed by the experimental findings (Fig. 1b and 1c).

While conducted on different days, the SE and LIBRE-Iso3DGRE T_2 maps obtained from phantom experiments agreed well (Figure 2a and 2b). A high coefficient of determination (R^2=0.99) and a good agreement ($T_{2LIBRE\text{-}Iso3DGRE}=0.93\times T_{2SE}+0.11$ms, P=0.0002, Figure 2c) was found between LIBRE-Iso3DGRE T_2 values and the gold standard SE values

when the empirical fit offset δ was set to 2.0ms. The T_2 values obtained with LIBRE-Iso3DGRE ranged from 23.8±1.0ms to 46.3±1.5ms, while those obtained with the gold standard varied from 26.0±1.0ms to 49.4±1.6ms. While there was a small underestimation (linear fit slope=0.93±0.04), a negligibly small fit intercept was found (0.11±1.64ms), as expected given the use of the empirical fit offset. The relation between SE and LIBRE-Iso3DGRE T_2 values could therefore be considered directly proportional, as was previously demonstrated for SE and Iso3DGRE T_2 values (14). The Bland-Altman analysis resulted in a bias of -2.7ms with a 95% confidence interval of ±1.9ms (Figure 2d).

Phantom T_2 values obtained with LIBRE-Iso3DGRE were slightly higher than those obtained with the Iso3DGRE T_2 mapping technique. Given the negligible fit intercept of 0.005±1.57ms, the linear regression analysis resulted in a relationship directly proportional ($T_{2\text{LIBRE-Iso3DGRE}}=1.03\times T_{2\text{Iso3DGRE}}$, $R^2=0.99$, P=0.0002, Figure 2e). The Bland-Altman bias was 1.0ms and the 95% confidence interval was ±1.3ms (Figure 2f).

Water signal was not lost due to the off-resonance LIBRE excitation (SNR=25.5 vs. SNR=19 for spectral fat saturation and SNR=26 for conventional WE, Supplementary Figure 2a) while it allowed for improved fat signal suppression (SNR=12) than conventional water excitation (SNR=40) and spectral fat saturation (SNR=18, Supplementary Figure 2b).

In vivo studies

In vivo, CS artifacts were no longer detectable (completely absent) when using LIBRE pulses (Fig. 3a-h).

Averaged over all subjects, the LIBRE-Iso3DGRE T_2 values (36.5±2.9ms) were slightly but not significantly higher than those determined with Iso3DGRE (34.1±5.1ms, P=0.1),

similar to what was observed in the phantom studies. The Bland-Altman analysis resulted in a bias of 2.4ms with a 95% confidence interval of 7.1ms. In each compartment, the difference between T_2 values obtained with LIBRE-Iso3DGRE and Iso3DGRE was not significant, except for the tibial lateral and femoral lateral anterior compartment (P=0.008 and P=0.006, respectively), as well as for the femoral medial posterior compartment (P=0.03).

Overall, both LIBRE-Iso3DGRE and Iso3DGRE cartilage T_2 maps showed similar anatomical patterns. The main differences could be found at the cartilage-bone interface (Fig. 4a-n). Here, CS artifacts caused a hyperintense layer of pixels in the images (Fig. 4b and 4h) that resulted in a thin layer of high T_2 values in the maps (Fig. 4f and 4n), while these CS artifacts were absent in the LIBRE-Iso3DGRE maps (Fig. 4a and 4g).The LIBRE pulse allowed for more precise T_2 estimation, as confirmed by a decrease in the relative T_2 standard deviation (averaged over all compartments and volunteers) from 30.5±9.9% for Iso3DGRE to 23.7±7.4% for LIBRE-Iso3DGRE (P<0.0001).

Averaged over all healthy volunteers, the reduction of fat SNR in the femoral bone marrow and infrapatellar fat pad was 86.4±2.4% when using a LIBRE pulse.

The LIBRE-Iso3DGRE pulse sequence resulted in significantly lower SAR when compared to its non-fat suppressed counterpart for the healthy volunteer studies (0.063±0.005W/Kg for LIBRE-Iso3DGRE and 0.079±0.007W/Kg for Iso3DGRE, p<0.0001).

DISCUSSION

In this study we sought to combine a recently developed isotropic 3D T_2 mapping technique with a novel robust and short water excitation RF pulse for improved knee

cartilage evaluation. Cartilage delineation and T_2 map precision were improved by using the new lipid insensitive T_2 mapping technique that was devoid of CS artifacts resulting from nearby lipid signals.

The LIBRE pulse was optimized by means of numerical simulations and was then combined with the Iso3DGRE T_2 mapping technique. The fat suppression characteristics obtained using a short 1ms total pulse duration were consistent with previously reported results (21) with pulse durations between 1.4ms and 2.6ms.

This lipid insensitive technique was then tested and validated in vitro. Phantom T_2 values were compared with those obtained with the gold standard SE and a high correlation was found. The comparison between T_2 values obtained with Iso3DGRE with normal excitation and with the LIBRE pulse showed a direct proportionality and a slight trend of overestimation by LIBRE-Iso3DGRE.

In vivo, T_2 maps of knee cartilage in seven healthy volunteers were obtained with both techniques. The average LIBRE-Iso3DGRE T_2 values were higher than those obtained with Iso3DGRE, and the corresponding Bland-Altman bias of 2.4ms was consistent with the overestimation trend observed in phantoms. In both cases, the empirical fit offset δ was carefully chosen in order to minimize the intercept value in the linear regressions with the SE technique (14). The two T_2 mapping methods are characterized by a slightly different timing and T_1 relaxation contributions, which most likely caused the small differences in T_2 values. The robust and homogeneous fat suppression obtained with the short LIBRE pulse prevented CS artifacts from fatty subchondral bone marrow that were responsible for a thin lamina of high T_2 values at the cartilage-bone interface (10) in the technique without fat suppression. The absence of this high T_2 layer might be the reason

why the LIBRE pulse used in this study allowed for more precise T_2 estimation (i.e. lower relative standard deviation) when compared with standard excitation.

In general, knee cartilage T_2 mapping suffers from the presence of volume averaging and chemical shift artifacts (33) that might affect the goodness of T_2 quantification in terms of accuracy and precision. The submillimetric isotropic resolution (i.e. 0.6mm) obtained with the present technique limited the partial volume artifacts that could arise from the volumetric signal averaging of bone and cartilage at their interface. CS artifacts, despite having a minimal effect on cartilage thickness measurements with GRE-based pulse sequences (34), may still cause phase-cancellation and misregistration or shadowing effects in Iso3DGRE T_2 mapping (14).

Uniform fat suppression - particularly challenging due to the complex magnetic environment that characterizes musculoskeletal imaging - was therefore achieved by using the LIBRE pulse (21). The LIBRE-Iso3DGRE acquisition time was one minute longer compared to Iso3DGRE (11.1 vs. 10.1 minutes, +10%). Moreover, given the longer pulse duration and therefore lower RF pulse amplitude, the LIBRE-Iso3DGRE pulse sequence resulted in significantly lower SAR when compared to its non-fat suppressed counterpart for the healthy volunteer studies. If conventional WE (a 1-180°-1 pulse (31)) or fat saturation (19) techniques were used in combination with the Iso3DGRE technique, they would result in a similar increase in acquisition time: +20% for the WE and +6% for the fat saturation pulse (data not shown). However, both methods produced heterogeneous and less effective fat suppression.

Note that to avoid CS artifacts, water excitation methods may be preferred over spectral fat saturation, because fat signal recovery due to T_1 cannot be neglected when acquisitions are performed using a large number of segments as was the case in this

study. However, the shortest binomial water excitation pulse (1-180°-1), which consists of two RF pulses with a fixed inter-pulse delay chosen to allow 180° of phase evolution between water and fat spins (i.e. 1.1ms at 3T) has a total RF pulse duration of approximately 1.7ms at 3T and has a relatively narrow fat suppression bandwidth (31,35). Dixon (36) or inversion-based fat suppression techniques were not considered in this study due to their intrinsic long imaging time (17) that is not suited for T_2 mapping techniques.

Several factors may pose limitations to the present study. First, the influence of incidental magnetization transfer, diffusion, modulation of k-space across the excitations per segment, and magic angle effects on the T_2 estimation were not investigated. Second, the cartilage ROIs were manually segmented - this approach was naturally less reproducible in determining the cartilage-bone interface than using an automated segmentation routine that would have reduced observer bias in determining cartilage boundaries. Third, since the LIBRE sub-pulses are not spatially selective, aliasing artifacts were observed in the left-right phase encoding direction. Increasing the matrix size in this direction would have circumvented this limitation, but at the expense of longer acquisition time. However, artifacts arose near the edges outside the FOV and did not affect the segmentation of cartilage in the central regions of the lateral and medial condyles. Fourth, the proposed sequence will not assess the bound-water components of cartilage, which have T_2* values on the order of 0.5-0.8ms (37) (38) and will have a negligible contribution to the signal at TE=2.1-3.2ms compared to that of the unbound water. Furthermore, as opposed to menisci and ligaments, the bound water fraction of cartilage, is not predominant and accounts only for 15.2-18.5% (37,38) of the water. At the different TEs, the short-T_2 component therefore causes a negligible difference of 0.26% in our T_2 quantification. The

analysis of the short T2 components of cartilage requires specific quantification techniques, such as ultrashort echo time (UTE) techniques (39).

The study design itself also has several limitations. First, the number of analyzed healthy subjects was small. Second, no patient studies were included and therefore the ability to visualize abnormalities was not assessed.

Future developments may focus on the application of this technique in a specific patient population or other body parts. Possible applications include the ankle and the hip (albeit with adaptations to accommodate for fold-over effects) is foreseeable. The flexible and variable parameter space of the LIBRE pulse could be further exploited in order to decrease its total duration. However, a shorter pulse duration will result in increased RF pulse amplitude and an increased f_{RF} (and therefore farther off-resonance excitation). Both these effects will cause SAR growth, which would necessitate a longer recovery time in compensation. Finally, an automated or semi-automated routine may be added in order to reduce operator bias in cartilage segmentation and compressed sensing (40) may be used to decrease the acquisition time.

In conclusion, it was demonstrated that a LIBRE RF excitation pulse as short as 1ms can be successfully combined with a 0.6-mm isotropic 3D GRE T_2 mapping technique for quantitative knee cartilage evaluation. Homogeneous and robust LIBRE fat signal suppression allowed for the removal of CS artifacts and resulted in improved cartilage delineation and more precise T_2 values.

REFERENCES

1. Lawrence RC, Felson DT, Helmick CG, et al. Estimates of the prevalence of arthritis and other rheumatic conditions in the United States. Part II. Arthritis Rheum 2008;58(1):26-35.

2. Cross M, Smith E, Hoy D, et al. The global burden of hip and knee osteoarthritis: estimates from the global burden of disease 2010 study. Annals of the rheumatic diseases 2014;73(7):1323-1330.

3. Guermazi A, Crema MD, Roemer FW. Compositional Magnetic Resonance Imaging Measures of Cartilage--Endpoints for Clinical Trials of Disease-modifying Osteoarthritis Drugs? J Rheumatol 2016;43(1):7-11.

4. Roemer FW, Crema MD, Trattnig S, Guermazi A. Advances in imaging of osteoarthritis and cartilage. Radiology 2011;260(2):332-354.

5. David-Vaudey E, Ghosh S, Ries M, Majumdar S. T2 relaxation time measurements in osteoarthritis. Magn Reson Imaging 2004;22(5):673-682.

6. Mamisch TC, Trattnig S, Quirbach S, Marlovits S, White LM, Welsch GH. Quantitative T2 mapping of knee cartilage: differentiation of healthy control cartilage and cartilage repair tissue in the knee with unloading--initial results. Radiology 2010;254(3):818-826.

7. Apprich S, Mamisch TC, Welsch GH, et al. Quantitative T2 mapping of the patella at 3.0T is sensitive to early cartilage degeneration, but also to loading of the knee. Eur J Radiol 2012;81(4):e438-443.

8. Kijowski R, Blankenbaker DG, Munoz Del Rio A, Baer GS, Graf BK. Evaluation of the articular cartilage of the knee joint: value of adding a T2 mapping sequence to a routine MR imaging protocol. Radiology 2013;267(2):503-513.

9. Dunn TC, Lu Y, Jin H, Ries MD, Majumdar S. T2 relaxation time of cartilage at MR imaging: comparison with severity of knee osteoarthritis. Radiology 2004;232(2):592-598.

10. Smith HE, Mosher TJ, Dardzinski BJ, et al. Spatial variation in cartilage T2 of the knee. J Magn Reson Imaging 2001;14(1):50-55.

11. Welsch GH, Scheffler K, Mamisch TC, et al. Rapid estimation of cartilage T2 based on double echo at steady state (DESS) with 3 Tesla. Magn Reson Med 2009;62(2):544-549.

12. Heule R, Ganter C, Bieri O. Triple echo steady-state (TESS) relaxometry. Magn Reson Med 2014;71(1):230-237.

13. Pai A, Li X, Majumdar S. A comparative study at 3 T of sequence dependence of T2 quantitation in the knee. Magn Reson Imaging 2008;26(9):1215-1220.

14. Colotti R, Omoumi P, Bonanno G, Ledoux JB, van Heeswijk RB. Isotropic three-dimensional T2 mapping of knee cartilage: Development and validation. J Magn Reson Imaging 2018;47(2):362-371.

15. Notohamiprodjo M, Horng A, Pietschmann MF, et al. MRI of the knee at 3T: first clinical results with an isotropic PDfs-weighted 3D-TSE-sequence. Invest Radiol 2009;44(9):585-597.

16. Van Dyck P, Gielen JL, Vanhoenacker FM, et al. Diagnostic performance of 3D SPACE for comprehensive knee joint assessment at 3 T. Insights into imaging 2012;3(6):603-610.

17. Del Grande F, Santini F, Herzka DA, et al. Fat-suppression techniques for 3-T MR imaging of the musculoskeletal system. Radiographics 2014;34(1):217-233.

18. Bydder GM, Pennock JM, Steiner RE, Khenia S, Payne JA, Young IR. The short TI inversion recovery sequence--an approach to MR imaging of the abdomen. Magn Reson Imaging 1985;3(3):251-254.

19. Haase A, Frahm J, Hanicke W, Matthaei D. 1H NMR chemical shift selective (CHESS) imaging. Phys Med Biol 1985;30(4):341-344.

20. Kaldoudi E, Williams SC, Barker GJ, Tofts PS. A chemical shift selective inversion recovery sequence for fat-suppressed MRI: theory and experimental validation. Magn Reson Imaging 1993;11(3):341-355.

21. Bastiaansen JAM, Stuber M. Flexible water excitation for fat-free MRI at 3T using lipid insensitive binomial off-resonant RF excitation (LIBRE) pulses. Magn Reson Med 2018;79(6):3007-3017.

22. Bloch F. Nuclear Induction. Phys Rev 1946;70:460-474.

23. Gold GE, Han E, Stainsby J, Wright G, Brittain J, Beaulieu C. Musculoskeletal MRI at 3.0 T: relaxation times and image contrast. AJR Am J Roentgenol 2004;183(2):343-351.

24. Nezafat R, Stuber M, Ouwerkerk R, Gharib AM, Desai MY, Pettigrew RI. B1-insensitive T2 preparation for improved coronary magnetic resonance angiography at 3 T. Magn Reson Med 2006;55(4):858-864.

25. van Heeswijk RB, Feliciano H, Bongard C, et al. Free-breathing 3 T magnetic resonance T2-mapping of the heart. JACC Cardiovasc Imaging 2012;5(12):1231-1239.

26. van Heeswijk RB, Piccini D, Feliciano H, Hullin R, Schwitter J, Stuber M. Self-navigated isotropic three-dimensional cardiac T2 mapping. Magn Reson Med 2015;73(4):1549-1554.

27. Bano W, Feliciano H, Coristine AJ, Stuber M, van Heeswijk RB. On the accuracy and precision of cardiac magnetic resonance T2 mapping: A high-resolution radial study using adiabatic T2 preparation at 3 T. Magn Reson Med 2017;77(1):159-169.

28. Pell GS, Briellmann RS, Waites AB, Abbott DF, Lewis DP, Jackson GD. Optimized clinical T2 relaxometry with a standard CPMG sequence. J Magn Reson Imaging 2006;23(2):248-252.

29. Griswold MA, Jakob PM, Heidemann RM, et al. Generalized autocalibrating partially parallel acquisitions (GRAPPA). Magn Reson Med 2002;47(6):1202-1210.

30. Dietrich O, Raya JG, Reeder SB, Reiser MF, Schoenberg SO. Measurement of signal-to-noise ratios in MR images: influence of multichannel coils, parallel imaging, and reconstruction filters. J Magn Reson Imaging 2007;26(2):375-385.

31. Meyer CH, Pauly JM, Macovski A, Nishimura DG. Simultaneous spatial and spectral selective excitation. Magn Reson Med 1990;15(2):287-304.

32. Bland JM, Altman DG. Statistical methods for assessing agreement between two methods of clinical measurement. Lancet 1986;1(8476):307-310.

33. Mosher TJ, Dardzinski BJ. Cartilage MRI T2 relaxation time mapping: overview and applications. Semin Musculoskelet Radiol 2004;8(4):355-368.

34. McGibbon CA, Bencardino J, Palmer WE. Subchondral bone and cartilage thickness from MRI: effects of chemical-shift artifact. MAGMA 2003;16(1):1-9.

35. Bernstein MA, King KF, Zhou XJ. Handbook of MRI pulse sequences. Elsevier 2004.

36. Dixon WT. Simple proton spectroscopic imaging. Radiology 1984;153(1):189-194.

37. Pauli C, Bae WC, Lee M, et al. Ultrashort-echo time MR imaging of the patella with bicomponent analysis: correlation with histopathologic and polarized light microscopic findings. Radiology 2012;264(2):484-493.

38. Du J, Diaz E, Carl M, Bae W, Chung CB, Bydder GM. Ultrashort echo time imaging with bicomponent analysis. Magn Reson Med 2012;67(3):645-649.

39. Omoumi P, Bae WC, Du J, et al. Meniscal calcifications: morphologic and quantitative evaluation by using 2D inversion-recovery ultrashort echo time and 3D ultrashort echo time 3.0-T MR imaging techniques--feasibility study. Radiology 2012;264(1):260-268.

40. Huang C, Graff CG, Clarkson EW, Bilgin A, Altbach MI. T2 mapping from highly undersampled data by reconstruction of principal component coefficient maps using compressed sensing. Magn Reson Med 2012;67(5):1355-1366.

TABLES

Table 1. Pulse sequence parameters used in this study. The left and middle optimized parameter sets were used both in vivo and in vitro, while the right parameter set was only used during optimization of f_{RF} in vitro.

Sequence parameters	LIBRE-Iso3DGRE	Iso3DGRE	Low-Res LIBRE-Iso3DGRE
Slices (-)	144	144	48
RF pulse duration (ms)	1.0	0.3	1.0
Phase encoding directions	Left/Right Anterior/Posterior	Left/Right Anterior/Posterior	Left/Right Anterior/Posterior
Repetition time (ms)	7.1	5.2	4.8
Echo time (ms)	3.2	2.1	2.2
T_2 preparation durations (ms)	0, 23, 38, 53	0, 23, 38, 53	53
Receiver bandwidth (Hz/px)	301	301	445
Phase partial Fourier (-)	-	-	-
Slice partial Fourier (-)	¾	¾	¾
Matrix size (-)	272 × 280 ×144	272 × 280 ×144	96 × 92 × 48

Acquired voxel volume (mm^3)	0.63 × 0.63 × 0.63	0.63 × 0.63 × 0.63	1.56 × 1.56 x 3
GRAPPA factor* (-)	2×	2×	-
Scan time (min)	11.1	10.1	0.3

* GRAPPA applied in the phase encoding direction.

FIGURES

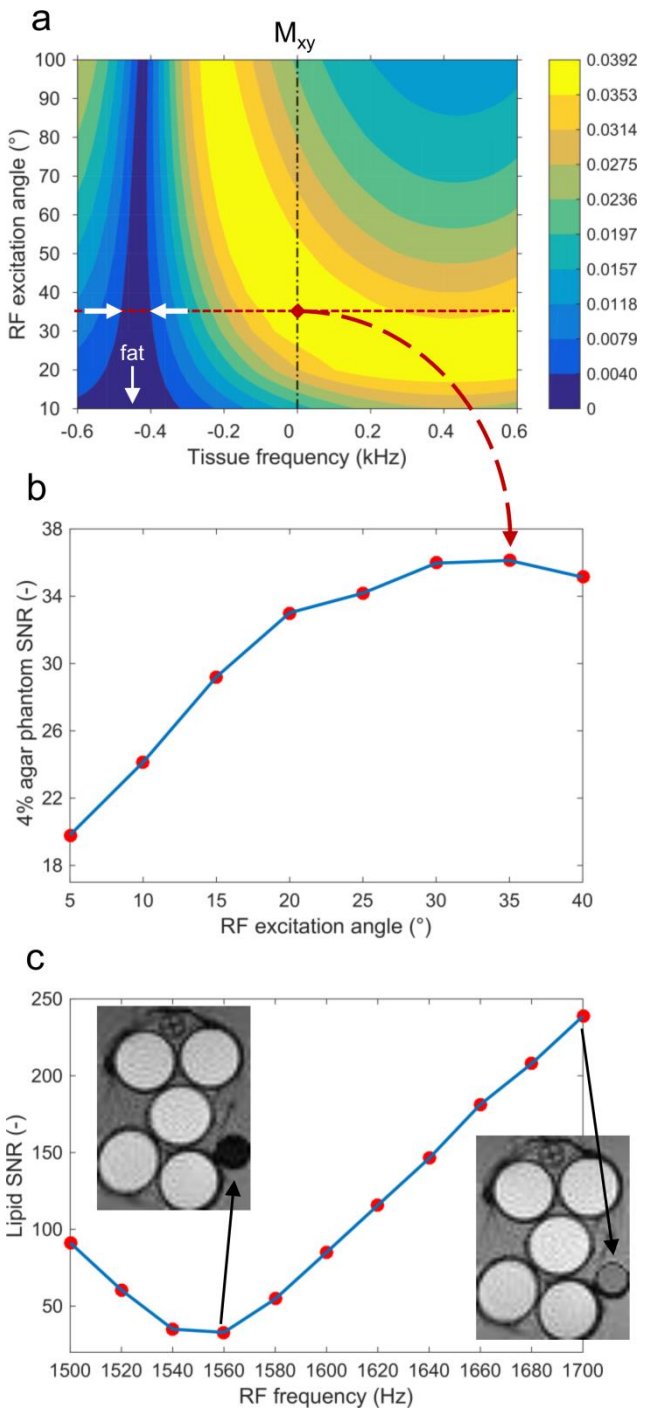

Figure 1. LIBRE pulse optimization for Iso3DGRE imaging of the knee. a) Simulation of the transverse magnetization M_{xy} following a T_2 preparation module (TE_{T2prep}=53ms) and LIBRE pulses as a function of tissue frequency and RF excitation angle α. The

horizontal axis was centered at 0Hz on the water resonance frequency, with -440Hz (white arrow) representing the resonance frequency of fat (at 3T). The red dotted line indicates α=35°, which allowed for simultaneous maximum water excitation and fat suppression. The fat suppression bandwidth was ~100Hz (white arrows). **b)** The SNR in the 4% agar phantom was plotted against α. The maximum (and thus optimal) SNR occurred at α=35°, in accordance with the findings from the numerical simulations. **c)** The SNR in the baby oil phantom that mimicked the magnetic properties of fat was plotted against the RF frequency offset (f_{RF}). The minimum (and thus optimal) SNR occurred at f_{RFopt}=1560Hz, as determined by (Eq.1). The insets show uniform (f_{RF}=1560Hz) and suboptimal (f_{RF}=1700Hz) fat suppression.

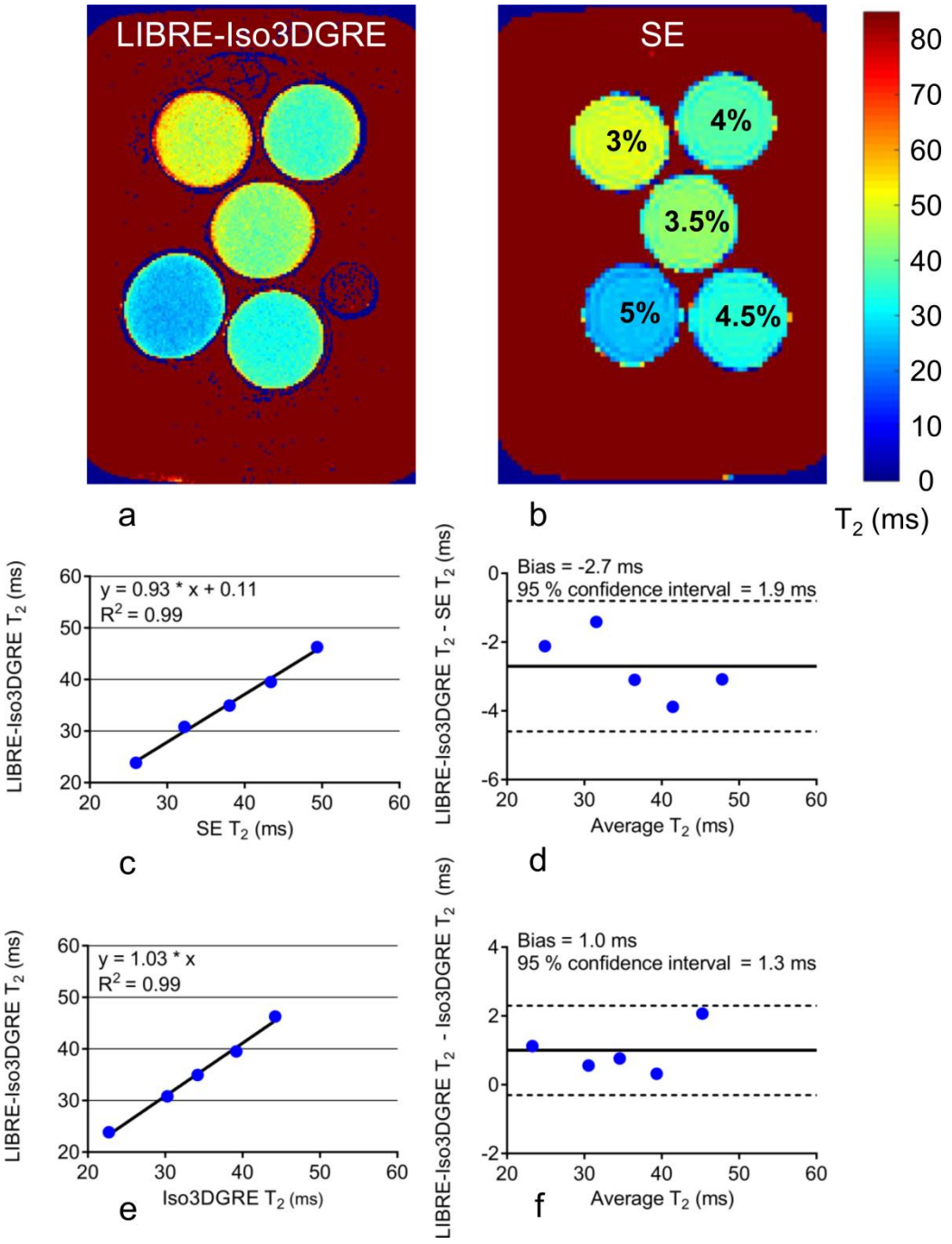

Figure 2. In vitro comparison between LIBRE-Iso3DGRE, SE and Iso3DGRE T_2 mapping techniques in a phantom containing five agar-$NiCl_2$ tubes. The percentage of agar is indicated in the SE T_2 map. Note that the phantom arrangement is slightly different. **a)** LIBRE-Iso3DGRE and **b)** SE T_2 map of the agar phantoms. **c)** Even if LIBRE-

Iso3DGRE T_2 mapping underestimates the SE T_2 values (linear fit slope=0.93±0.04), the relationship between the T_2 values obtained with the two techniques is directly proportional (linear fit intercept=0.11±1.6). **d)** The LIBRE-Iso3DGRE T_2 mapping technique resulted in a bias of -2.7ms and 95% confidence interval of ±1.9ms. **e)** The linear regression of the LIBRE-Iso3DGRE T_2 values with the Iso3DGRE T_2 values resulted in a perfect direct proportionality, as indicated by a linear fit intercept of zero in the regression equation. **f)** The Bland-Altman analysis of the phantom studies between the Iso3DGRE T_2 mapping technique with and without LIBRE pulse resulted in a bias of 1.0ms and 95% confidence interval of ±1.3ms.

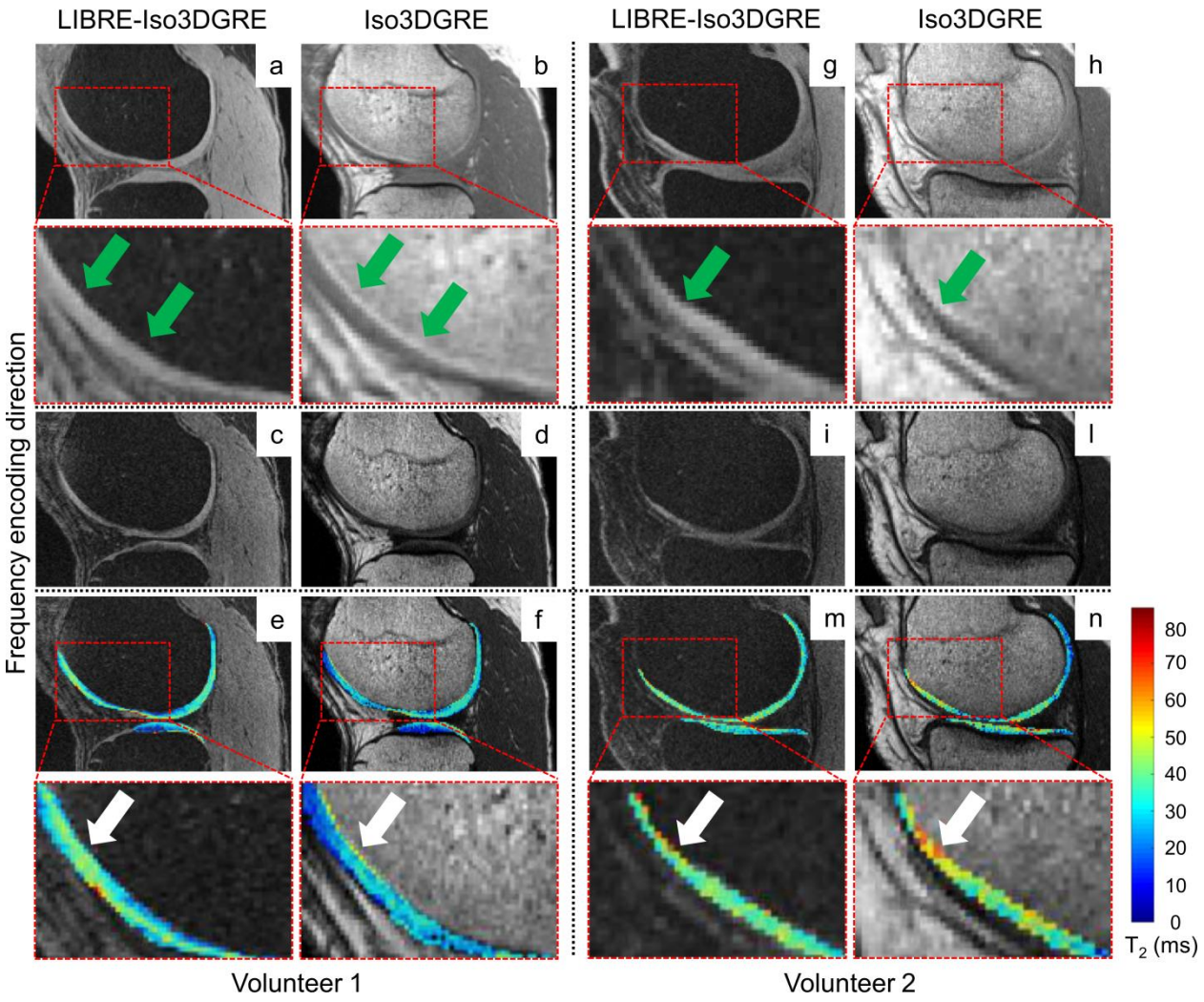

Figure 3. LIBRE-Iso3DGRE and Iso3DGRE sagittal slices spanning from the lateral to the medial condyle in a healthy volunteer. Both **a-d)** LIBRE-Iso3DGRE and **e-h)** Iso3DGRE images were obtained with TE_{T2prep}=0ms. The signal arising from the fat tissue around the joint (orange arrows) was suppressed as well as the signal from the fatty subchondral bone marrow that caused the appearance of CS artifacts at the interface between cartilage and subchondral bone (black arrows). The fat suppression was homogeneous (blue arrows) and consequent improved cartilage delineation was obtained with the LIBRE pulse at the expense of only +10% of the acquisition time than normal

excitation. Despite a visual signal intensity difference, the SNR from the muscle tissue was the same for both LIBRE-Iso3DGRE and Iso3DGRE techniques.

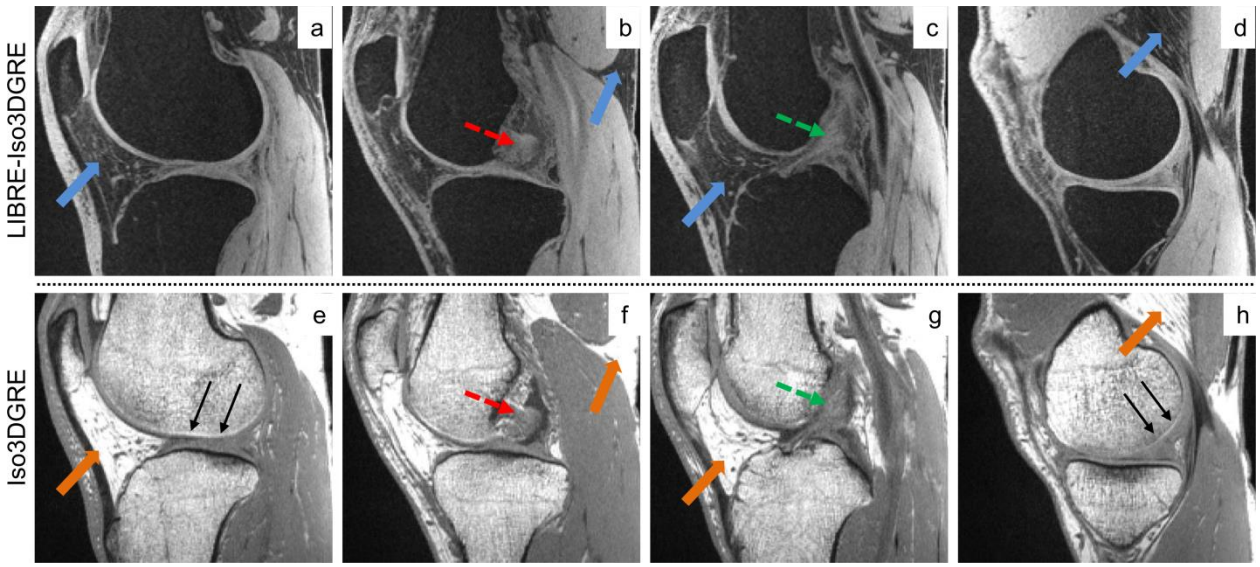

Figure 4. Representative medial LIBRE-Iso3DGRE and Iso3DGRE input images and T_2 maps in two healthy volunteers. a, g) Input images (TE_{T2prep}=0ms) obtained with the LIBRE-Iso3DGRE and **b, h)** the Iso3DGRE technique. Note that the window/level settings are different in order to allow for anatomical visualization and optimal cartilage segmentation. The zoomed-in region demonstrates the absence of CS artifacts, as opposed to the Iso3DGRE image (green arrows). **c, i)** LIBRE-Iso3DGRE and **d, l)** Iso3DGRE input images obtained with TE_{T2prep}=23ms were used for cartilage segmentation. **e, m)** LIBRE-Iso3DGRE and **f, n)** Iso3DGRE T_2 maps overlaid on related morphological images. In the Iso3DGRE image, the white arrow indicates the effect of CS artifacts on T_2 value estimation (higher values).